THE JOURNAL OF PHYSICAL CHEMISTRY Letters

Letter

Cite This: J. Phys. Chem. Lett. 2018, 9, 5023−5028

pubs.acs.org/JPCL

Self-Phoretic Microswimmers Propel at Speeds Dependent upon an Adjacent Surface's Physicochemical Properties

Andrew Leeth Holterhoff,[†,‡] Mingyang Li,[†,‡] and John G. Gibbs*[,†]

[†]Department of Physics and Astronomy, Northern Arizona University, Flagstaff, Arizona 86011, United States

ABSTRACT: Self-phoretic colloids are emerging as critical components of programmable nano- and microscale active matter and may usher in a new area of complex, small-scale machinery. To date, most studies have focused upon active particles confined by gravity to a plane located just above a solid/liquid interface. Despite this ubiquity, little attention has been directed at how the physicochemical qualities of this interface might affect motion. Here, we show that both the chemical and physical properties of the solid, above which motion takes place, significantly influence the behavior of particles propelled by self-generated concentration gradients. More specifically, titania/silica (TiO_2/SiO_2) photoactive microswimmers move faster when the local osmotic flow over the stationary solid is diminished, which we demonstrate by reducing the magnitude of the surface's zeta potential or by increasing surface roughness. Our results suggest that consideration of surface properties is crucial for modeling self-phoretic active matter while simultaneously offering a new avenue for engineering the kinematic behavior of such systems.

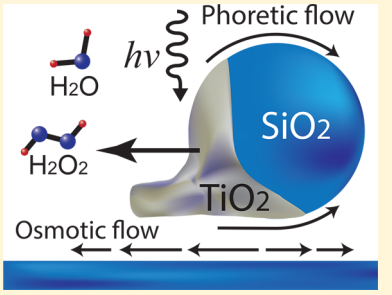

Nonequilibrium active particles,[1] droplets,[2] and molecules[3,4] are expected to be the ingredients of future micro- and nanomachines[5,6] capable of performing detailed tasks at very small scales, highlighting the need for developing advanced systems of this type[7−10] that can simultaneously provide new insight about how such systems operate.[11,12] Much remains unknown about the intricacies of microscale active motion, which may be especially true for particles that undergo self-propulsion via localized chemical concentration gradients.[13−15] Further complicating the understanding of the behavior of such systems arises when microswimmers move near boundaries, such as other particles[16] or walls,[12,17,18] as many do. However, a flurry of research has led to significant progress on this topic of late,[19,20] and furthermore, we may be able to turn this complication into an asset in the following way: If the swimming behavior changes as a function of the immobile surface's properties, new opportunities for controlling motion at the microscale are expected to arise. In this study, we show that photoactivated catalytic microswimmers made from titanium dioxide (TiO_2) and silicon dioxide (SiO_2)[21−23] move at speeds dependent upon the physicochemical properties of an adjacent surface. The microswimmers propel at disparate average speeds when traversing surfaces of different materials; here we show that motion is ∼25% faster over gold (Au) vs SiO_2. We also observe changes in speed when the material is held constant but the surface roughness is altered. We suspect that our observations arise from surface-dependent osmotic flow in the electrical double layer above the stationary solid, which links back to the nearby microswimmer, consequently affecting its overall dynamics.

The way in which a nearby surface influences the motive behavior of a particular self-propelled microswimmer is intricately related to its mechanism of motion,[24] which may lead to self-assembly[25,26] and aggregation at boundaries,[27,28] and in special cases, the walls may even be responsible for the active motion itself.[29] Here, we are interested in catalytic microswimmers that gain self-propelled mobility resulting from a chemical reaction taking place on the particle's surface.[30,31] More specifically to this study, the reaction is light-activated, made possible by constructing the swimmers from a photocatalyst.[23] To date, the majority of studies on this topic have investigated particles moving just above the interface forming the boundary between a stationary bottom solid surface and the liquid through which the particles swim on the top. This is true for two reasons: (1) the particles are heavy and therefore sink to the interface under the effect of gravity and (2) after settling remain mostly confined to a single plane, allowing for practical observation via optical microscopy. Because a catalytic microswimmer moves as a result of self-generated local chemical concentration gradients, which induce flow over the swimmer and consequential self-propulsion, when moving near a solid boundary, these same gradients can also activate chemiosmotic flow at that interface.[32] This secondary fluid motion may couple significantly to the nearby particle, potentially leading to marked changes in its dynamics. By extension, because the way that any submerged surface responds to a concentration gradient depends on its physicochemical properties, it would be reasonable to imagine that surface modification could give rise to appreciable changes in microswimmer behavior due to this coupling. Our aim is to investigate this effect, for which only a very limited amount of experimental evidence currently exists,[33,34] by observing surface-dependent motion of two distinct photoactive TiO_2/SiO_2 microswimmer morphologies: the Janus[35−37] sphere and

Received: July 23, 2018
Accepted: August 18, 2018
Published: August 19, 2018

DOI: 10.1021/acs.jpclett.8b02277
J. Phys. Chem. Lett. 2018, 9, 5023−5028

an elongated Janus particle with a photocatalytic "tail", as shown in Figure 1a,b, respectively. The particles propel above

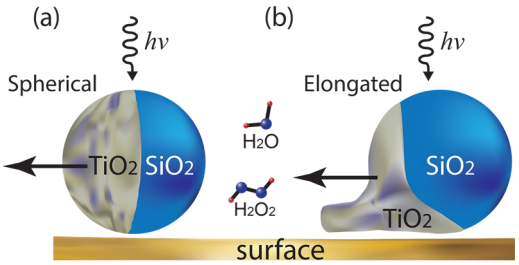

Figure 1. Schematic showing two morphologies of photoactive TiO_2/SiO_2 Janus microswimmers moving just above a solid surface in H_2O_2 and H_2O: (a) spherical and (b) elongated Janus particles with photoactive tails. When UV light is present, photolysis of H_2O_2 on the surface of the titania leads to the microswimmers translating toward the active segments.

the solid surface toward the photoactive TiO_2 portions, indicated by the arrows in Figure 1, in hydrogen peroxide (H_2O_2) and water, while exposed to ultraviolet (UV) light.

We start by comparing motion over surfaces of either SiO_2 or Au. For each experiment, we measure the speeds of at least 75 distinct particles, and the results are represented by the probability distributions in Figure 2a for Janus spheres and Figure 2b for asymmetric elongated Janus microswimmers (see the Experimental Section for details of how the data was obtained and processed). The narrow light blue and diagonal striped black bars represent the chance of measuring a particle with a particular range of speeds moving over SiO_2 or Au, respectively. Note that the former have been artificially narrowed for clarity but in reality span the same 1 μm/s range as the wide bars. The insets in Figure 2 allow one to quickly reference the experimental conditions that led to each plot, i.e., surface- and particle-type. A point of potential interest is the generally much higher speeds of the elongated (Figure 2b) vs spherical Janus particles (Figure 2a), which is consistent with our earlier results.[23] On average, both particle types moved ~25% faster over Au: for spherical, $\overline{v}_{Sp,SiO_2} = 3 \pm 1$ μm/s, $\overline{v}_{Sp,Au} = 4 \pm 1$ μm/s; elongated, $\overline{v}_{E,SiO_2} = 22 \pm 5$ μm/s, $\overline{v}_{E,Au} = 27 \pm 9$ μm/s, where the subscripts Sp and E refer to spherical and elongated, respectively. Before moving forward, we'd like to articulate the rational for investigating two different microswimmer morphologies: Perhaps unsurprisingly, the purpose was to help clarify if the observed surface-dependent average speed is itself a function of particle shape. Our results in Figure 2 suggest that the effect may not be strongly shape-dependent, if at all. More importantly, the two different samples showing almost identical relative increases in speed is evidence of reproducibility.

Although the average speeds near surfaces of Au are higher than what is observed near SiO_2 for both particle types, the standard deviations obscure whether or not the average helps us extract any definitive conclusion. In order to quantify the significance of the difference between the average speeds over SiO_2 and Au, we performed an unpaired t-test, which gave p values of <0.0001 for spherical and 0.0003 for elongated particles, both of which indicate a high level of significance. We furthermore found the size of the effect of the substrate on particle speed to be $d_{Sp} \approx 0.9$ and $d_E \approx 0.6$ (Cohen's d),[38] for the spherical and elongated particles, respectively, indicating "medium" to "large" effect sizes. We additionally give a qualitative description of the results. The probabilities for the speeds of the Janus spheres shown in Figure 2a have a few notable characteristics: For the SiO_2 surface, we are most likely to measure a particle moving within the range of the slowest speeds $1.5 \leq v < 2.5$ μm/s, and indeed, a true majority, ~55%, fell into this bin. On the other hand, we have the highest chance of measuring a particle moving over Au in the slightly faster $2.5 \leq v < 3.5$ μm/s range, ~32%. As we look at the probabilities for even higher speeds than these first two intervals, we arrive at what is the most important feature: The chance of measuring a particular speed decays to zero more rapidly for the SiO_2 surface as we move along the horizontal axis in Figure 2a. Further, the highest speed measured over SiO_2 from a 190 point data set was $v = 5.8$ μm/s, while we found ~20% propelled faster than this value when moving atop Au. We note that the two fastest speeds for Au, ~14 and ~16 μm/s, which are not plotted in Figure 2a for clarity, are about

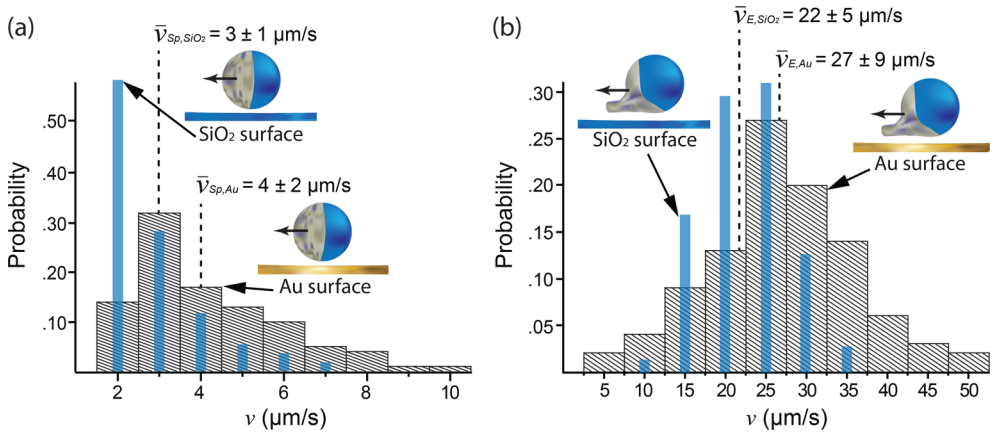

Figure 2. (a) Plot showing the probability distributions of measuring speeds for photoactive TiO_2/SiO_2 Janus spheres moving over SiO_2 or Au, shown as narrow light blue vertical bars and wide bars with black diagonal lines, respectively. Note that the blue vertical bars for the SiO_2 surface are artificially narrowed for clarity. (b) Probability distributions for the TiO_2/SiO_2 elongated microswimmers moving over SiO_2 or Au. The insets schematically illustrate the particle morphology and surface material, the latter of which is color-coded: blue for SiO_2 and golden for Au. Also shown in the insets are the average speeds, where the subscripts indicate the surface material and particle morphology: Sp represents spherical, and E represents elongated.

DOI: 10.1021/acs.jpclett.8b02277
J. Phys. Chem. Lett. 2018, 9, 5023−5028

2.5× faster than the quickest particle moving over SiO_2. We find similar trends for the elongated particles. The plot in Figure 2b indicates that the distributions for both surfaces are approximately normal, with some skewness, but the peak probability is shifted to faster speeds for Au, consistent with the higher average, while the distribution is simultaneously broader. Also mirroring the Janus sphere data, we find a significant number (~16%) of elongated particles moving over Au at speeds higher than the absolute fastest over SiO_2, ~35 μm/s.

One potentially simple explanation for the difference in speed for motion adjacent to the surfaces of disparate chemistry could arise from UV light reflecting more from Au, providing greater light intensity and consequential higher speeds.[21] However, gold is not particularly effective at reflecting wavelengths around λ = 365 nm, but the reflectance does increase with thickness.[39] If greater reflectance from the Au surface is the primary contributing factor for our observations, we would expect there to be a correlation between Au thickness and average speed. We tested this idea by measuring the speed of the Janus spheres moving over Au thin films of four thicknesses, 2.5, 10, 20, and 25 nm, as well as "0 nm", which corresponds to bare silica. The results are given in Table 1. Consistent with the data in Figure 2, the average speed for any Au surface was higher than the average for bare SiO_2, but we did not find any discernible correlation between speed and thickness, suggesting that increased reflection does not have a pronounced impact. This result also advances the idea that the observed material-dependent speed is a surface effect only, which if nothing else agrees with intuition.

Table 1. Average Speed of Janus Spheres vs Thin-Film Thickness of Au[a]

thickness (nm)	speed (μm/s)
0	3 ± 1
2.5	5 ± 3
10	4 ± 1
20	5 ± 3
25	4 ± 2

[a]Note that thickness = 0 nm corresponds to bare SiO_2.

In order to delve a little deeper into a possible mechanism, we take a closer look at the reaction taking place on a particle's photoactive surface. When exposed to UV light, the TiO_2 segment generates electron−hole pairs, UV + $TiO_2 \rightarrow TiO_2(h^+ + e^-)$,[40] greatly increasing the rate of the reaction $2H_2O_2 \rightarrow 2H_2O + O_2$ via photolysis, likely proceeding by two partial reactions

$$H_2O_2 + 2e^- + 2H^+ \rightarrow 2H_2O$$
$$H_2O_2 + 2h^+ \rightarrow O_2 + 2H^+ \quad (1)$$

which generate local concentration gradients of the reactant and its products. Although it is unclear if gradients of the neutral (H_2O_2, O_2) or charged (H^+) chemical species dominate in establishing the phoretic flow over the particle, which is responsible for self-propulsion, we suspect that there is at least some contribution from a gradient of the protons, H^+, or in other words, "self-electrophoresis" contributes.[41] If such a mechanism is at least partially responsible for motion, we expect higher solution conductivity, K, to decrease the average speed[42,43] as electrokinetic mobility scales inversely to the conductivity, $v \approx j\zeta_p\epsilon/\eta K$, where j, ζ_p, ϵ, and η are the proton current, zeta potential of the particle, permittivity, and viscosity of the fluid, respectively. To test this idea, we once again turn to the elongated microswimmers moving over SiO_2 but this time in a solution of 0.1 mM NaCl. With all other conditions held constant, i.e., H_2O_2 concentration and UV light intensity, the particles move in the salt solution at an average speed of 3 ± 1 μm/s, which is substantially slower than what is measured in water alone, 22 ± 5 μm/s (see Figure 2b). The slower speed in the salt solution hints that there is a self-electrophoretic component to the mechanism, but it should be noted that this observation does not necessarily mean that this mechanism dominates. In the following, we assume that self-electrophoresis does dominate for simplicity of argument.

Similar to the electrophoretic speed for the particle, electro-osmotic (EO) flow over the stationary surface is given by the well-known Helmholtz−Smoluchowski (HS) equation for the slip velocity $\vec{u} = -\zeta_w\epsilon/\eta\vec{E}$, where ζ_w is now the zeta potential of the wall and $\vec{E}$ is the electric field, which in this case is generated by the imbalance in the concentration of protons.[44] By accounting for both phoretic flow over the particle and EO flow over the stationary surface, we should be able to approximate the expected observed speed

$$\vec{v} \simeq \epsilon\frac{\zeta_p - \zeta_w}{\eta}\vec{E} \quad (2)$$

We assume that $\vec{E}$ remains unchanged despite altering the surface material (as discussed shortly, this may be a poor approximation) and assume that the field is a function of only the H_2O_2 concentration and light intensity, both of which were held constant. If we also assume that the properties of the fluid η and ϵ remain unchanged, then the zeta potential difference between the two surfaces would be the determining parameter. From the literature, at pH ≈ 7, the zeta potentials for Au and SiO_2 surfaces have been measured to be $\zeta_{w,Au} \approx -20$ mV[45] and $\zeta_{w,SiO_2} \approx -62$ mV,[46] respectively. For an increase in speed of ~1.25× when the particles are propelled over Au surfaces, as we observe, eq 2 tells us that the particles would need to have a zeta potential $\zeta_p \approx -225$ mV, which is unlikely to be accurate, as we expect the value to be somewhere in the range of $-20 < \zeta_p < 40$ mV.[47] This discrepancy is not surprising as eq 2 is an oversimplification of the system. For instance, eq 2 likely does not hold for conductive surfaces, and the $\vec{E}$ field is furthermore not uniform. In a previous study investigating a similar yet slightly different system to the one herein, i.e., self-electrophoretic Janus spheres in which a chemical is oxidized and reduced on two different electrically contacted electrodes, Chiang and Velegol showed by simulation that localized EO flow fields over a nearby wall affect such a particle's speed.[33] Importantly, the authors showed that the electric field generated by a self-propelled particle is significantly different from a typical uniform externally applied field, as is usually assumed in the HS equation. From that study, the critical parameter affecting speed is the ratio ζ_w/ζ_p. Because we expect ζ_w, $\zeta_p < 0$, according to these simulations, the condition $\zeta_{w,SiO_2} < \zeta_{w,Au}$ would lead to the particles moving faster over Au, as we observe. The rationale is that the osmotic flow over the stationary surface counteracts phoretic flow when ζ_w and ζ_p are the same sign, slowing the particle. Because the counteracting flow is slower over Au, the particles move faster over this surface.

DOI: 10.1021/acs.jpclett.8b02277
J. Phys. Chem. Lett. 2018, 9, 5023−5028

We note that a number of issues arise from our mostly qualitative explanation for our observations, with the most prominent being the following: (1) We do not know if the distance between the particles and the surface changes appreciably when we change materials. A constant distance was assumed in the above discussion regarding the ratio ζ_w/ζ_p being the determining factor.[33] (2) Another potential complication rests in the fact that Au is a catalyst for the breakdown of H_2O_2, which may alter the local concentration gradients. (3) The $\vec{E}$ field above the dielectric surface vs the conducting Au surface is likely to be significantly different, i.e., the field lines must be perpendicular to the conductive surface. For issue (1), if we assume that the distance does not change appreciably, the condition $\zeta_{w,SiO_2} < \zeta_{w,Au}$ may explain the result, but deriving a quantitative value to match our observations is impractical without knowing these distances. We suggest that direct measurement of this distance could be achieved by digital holography,[48] which is capable of high-resolution out-of-plane information. In order to address issues (2) and (3), we performed one additional experiment to bolster evidence that osmotic flow is the dominant factor determining the observed changes in speed. The idea is the following: if the osmotic flow can be suppressed in some other way besides changing the surface material (ζ_w) and if this leads to an *increase* in observed particle speeds, then the hypothesis would be supported.

It has been shown that increasing surface roughness impedes EO flow,[49,50] and therefore, we expect our microswimmers to move faster with increasing roughness despite the material remaining the same. We measured the speeds of ~100 elongated microswimmers moving over both smooth and rough surfaces of SiO_2. The smooth SiO_2 surfaces are thoroughly cleaned silica microscope slides, while the rough surfaces are produced by physically depositing 100 nm of SiO_2 onto a silica substrate at an oblique angle of 80°.[51−54] At this angle and deposition length, we expect the root-mean-square of the roughness to be ~5 nm.[55] We note that the data in Figure 3 for the smooth surface is different from that presented in Figure 2b in order to keep the experimental conditions as identical as possible. The data for motion over the rough vs smooth surfaces of SiO_2 in Figure 3 have some similarities to those comparing motion over SiO_2 vs Au (Figure 2b): We find a higher chance of measuring faster speeds for motion over the rough vs smooth surface, as expected, with averages of $\overline{v}_S$ = 21 ± 8 μm/s and $\overline{v}_R$ = 26 ± 10 μm/s, respectively. Also, the speeds of the fastest swimmers moving over the rough surface were significantly higher than those of the fastest moving over smooth SiO_2. Simple schematic representations of what we expect to be occurring are illustrated in the insets of Figure 3. For both rough and smooth SiO_2, EO flow, represented by the light blue arrows, counteracts the phoretic flow that gives rise to propulsion. However, for the rough surface, EO is partially impeded, and therefore, the counteraction is reduced, leading to higher observed speeds.

We have shown that the speeds of two distinct morphologies of photoactivated TiO_2/SiO_2 microswimmers is a function of the physicochemical properties of the surface over which they move. On average, the measured speeds change when either the zeta potential or the roughness of the surface is altered. This effect is reproducible and appears not to be strongly shape-dependent. Our results are consistent with a mechanism based upon surface-dependent osmotic flow at the stationary boundary that couples back to the nearby particles. Most self-phoretic particles investigated to date move near a solid/liquid interface, and here, we show that consideration of the surface physicochemical properties is important when investigating microswimmer dynamics. These results also suggest a new technique for modulating the behavior of self-phoretic colloids by modifying surface properties.

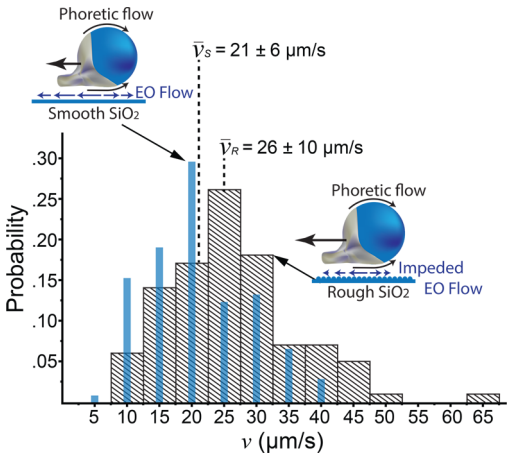

Figure 3. Probability distributions of measured speeds for elongated particles moving over smooth and rough surfaces of SiO_2. The narrow light blue and wide diagonal dashed black bars represent the probabilities of measuring speeds over smooth and rough surfaces, respectively. We expect the EO flow over the surfaces, shown in the insets, to reduce the observed speeds. EO flow is partially impeded over the rough surface, as indicated in the lower inset, which is expected to lead to faster speeds. The average speeds are indicated in the insets, and the subscripts "*S*" and "*R*" stand for smooth and rough, respectively.

EXPERIMENTAL SECTION

The underpinning of both microswimmer morphologies is an SiO_2 microsphere with an average diameter of 3.17 μm (Bangs Laboratories Inc., Fishers, IN). The photocatalyst TiO_2 (Kurt J. Lesker Company, Jefferson Hills, PA) was deposited via thermal evaporation onto close-packed, nearly monodisperse monolayers of these particles. To construct the Janus spheres, 50 nm of TiO_2 was deposited at a direction normal to the surface containing the monolayer, which led to a half-coating of the photocatalyst, as shown in Figure 1a. The structures with elongated tails, shown schematically in Figure 1b, resulted from depositing TiO_2 at an oblique angle of 85° to a thickness of ~1.5 μm.[23,56] After deposition, the particles were annealed at 500 °C for ~2 h in order to obtain the anatase crystalline phase of TiO_2, which is more photoactive than titania's other phases. The particles were mixed with hydrogen peroxide (H_2O_2) and water and were given enough time to settle to the solid/liquid interface. We carefully prepared the solid surfaces over which the particles moved because the purpose of this study is to explore the effect of those surfaces' properties upon the dynamics of the two photoactive microswimmer types. Silica microscope slides were first thoroughly washed with hot tap water and soap. Immediately after, the surfaces were liberally rinsed in deionized water followed by ethanol and then were dried with compressed nitrogen. A final cleaning step was performed by submitting the substrates to oxygen plasma. At this point, these slides were ready to be used in the experiments in which the active motors moved over silica. For

DOI: 10.1021/acs.jpclett.8b02277
J. Phys. Chem. Lett. 2018, 9, 5023−5028

the Au surfaces, we deposited onto silica slides, precleaned as detailed just above, 2.5 nm of titanium as an adhesion layer before depositing different amounts of gold by thermal evaporation. Afterward, the Au thin films were also further cleaned with plasma, but for this surface, we used argon to reduce the chance of oxidation. The particles were suspended in a colloid, which was pipetted into an observation cell, the bottom of which made up the surface of interest. The particles settled to that solid/liquid interface via gravity and were exposed to UV light at a peak wavelength of λ = 365 nm (Zeiss AxioScope.A1 fluorescence microscope). UV light was passed through a 40× objective while visible light was transmitted through the bottom of the glass cell. The motion of the particles was recorded with a Mikrotron EoSens GE Camera MC1364 at a frame rate of 11 fps. The videos were then processed via particle tracking, using the free software ImageJ with plugin MTrack2, in order to obtain two-dimensional trajectories of the swimmers. Microswimmers of both morphologies moved toward their titania segments, as indicated by the arrows in Figure 1a,b, at speeds that depend on the H_2O_2 concentration, the intensity of the activating light, and the properties of the surface over which motion takes place. In order to investigate the latter effect alone, we held the intensity and concentration constant at ∼0.5 W/cm^2 and 1% (v/v), respectively. The minimum number of particles measured was 75, and the maximum was 190. To calculate the speed of a single particle, we determined the distance traversed between subsequent frames and divided by 1/11 s (the frame rate used), and then, we averaged these values over all intervals of the particle's trajectory. Each particle was tracked for a minimum time of 5 s, and consequently, the minimum number of frames utilized to calculate the individual average speeds was ∼55. We note that speed fluctuates in systems such as the present one, and thereore, we corroborated our measurements against a second method that incorporates effects of diffusion, as detailed, for example, by Dunderdale et al.[57] We found that each method provided approximately the same speeds that fell within the standard deviation of the other. We furthermore note that the shape of the speed distributions may be affected by the time interval also resulting from speed fluctuations. However, we found that by reducing the interval, for example, to 2/11 s, the shape only slightly changed, preserving the prominent features of the data.

AUTHOR INFORMATION

Corresponding Author

*E-mail: john.gibbs@nau.edu.

ORCID

John G. Gibbs: 0000-0002-6510-9352

Author Contributions

‡A.L.H. and M.L. contributed equally to this work. A.L.H. and M.L. performed the experiments, analyzed data, contributed to the interpretation of the results, and wrote portions of the manuscript. J.G.G. conceived and managed the project, interpreted the results, and wrote the majority of the manuscript.

Notes

The authors declare no competing financial interest.

ACKNOWLEDGMENTS

This material is based upon work supported by the National Science Foundation under Grant No. CBET-1703322 and the Research Corporation for Science Advancement via the Cottrell Scholar Program. We also thank Prof. Wei Wang for his insightful comments regarding this project.

REFERENCES

(1) Aranson, I. S. Active colloids. *Phys.-Usp.* **2013**, *56*, 79.

(2) Tian, J.; Zhu, J.; Guo, H.-Y.; Li, J.; Feng, X.-Q.; Gao, X. Efficient self-propelling of small-scale condensed microdrops by closely packed ZnO nanoneedles. *J. Phys. Chem. Lett.* **2014**, *5*, 2084−2088.

(3) García-Iriepa, C.; Marazzi, M.; Zapata, F.; Valentini, A.; Sampedro, D.; Frutos, L. M. Chiral hydrogen bond environment providing unidirectional rotation in photoactive molecular motors. *J. Phys. Chem. Lett.* **2013**, *4*, 1389−1396.

(4) Hwang, W.; Hyeon, C. Energetic costs, precision, and transport efficiency of molecular motors. *J. Phys. Chem. Lett.* **2018**, *9*, 513−520.

(5) Ozin, G. A.; Manners, I.; Fournier-Bidoz, S.; Arsenault, A. Dream nanomachines. *Adv. Mater.* **2005**, *17*, 3011−3018.

(6) Ghosh, A.; Paria, D.; Rangarajan, G.; Ghosh, A. Velocity fluctuations in helical propulsion: How small can a propeller be. *J. Phys. Chem. Lett.* **2014**, *5*, 62−68.

(7) Yao, K.; Manjare, M.; Barrett, C. A.; Yang, B.; Salguero, T. T.; Zhao, Y. Nanostructured scrolls from graphene oxide for microjet engines. *J. Phys. Chem. Lett.* **2012**, *3*, 2204−2208.

(8) Suematsu, N. J.; Mori, Y.; Amemiya, T.; Nakata, S. Oscillation of speed of a self-propelled Belousov−Zhabotinsky droplet. *J. Phys. Chem. Lett.* **2016**, *7*, 3424−3428.

(9) Nourhani, A.; Brown, D.; Pletzer, N.; Gibbs, J. G. Engineering contactless particle−particle interactions in active microswimmers. *Adv. Mater.* **2017**, *29*, 1703910.

(10) Eßmann, V.; Voci, S.; Loget, G.; Sojic, N.; Schuhmann, W.; Kuhn, A. Wireless light-emitting electrochemical rotors. *J. Phys. Chem. Lett.* **2017**, *8*, 4930−4934.

(11) Nourhani, A.; Ebbens, S. J.; Gibbs, J. G.; Lammert, P. E. Spiral diffusion of rotating self-propellers with stochastic perturbation. *Phys. Rev. E: Stat. Phys., Plasmas, Fluids, Relat. Interdiscip. Top.* **2016**, *94*, 030601.

(12) Choudhury, U.; Straube, A. V.; Fischer, P.; Gibbs, J. G.; Höfling, F. Active colloidal propulsion over a crystalline surface. *New J. Phys.* **2017**, *19*, 125010.

(13) Paxton, W. F.; Sen, A.; Mallouk, T. E. Motility of catalytic nanoparticles through self-generated forces. *Chem. - Eur. J.* **2005**, *11*, 6462−6470.

(14) Velegol, D.; Garg, A.; Guha, R.; Kar, A.; Kumar, M. Origins of concentration gradients for diffusiophoresis. *Soft Matter* **2016**, *12*, 4686−4703.

(15) Theurkauff, I.; Cottin-Bizonne, C.; Palacci, J.; Ybert, C.; Bocquet, L. Dynamic clustering in active colloidal suspensions with chemical signaling. *Phys. Rev. Lett.* **2012**, *108*, 268303.

(16) Liebchen, B.; Marenduzzo, D.; Cates, M. E. Phoretic interactions generically induce dynamic clusters and wave patterns in active colloids. *Phys. Rev. Lett.* **2017**, *118*, 268001.

(17) Das, S.; Garg, A.; Campbell, A. I.; Howse, J.; Sen, A.; Velegol, D.; Golestanian, R.; Ebbens, S. J. Boundaries can steer active Janus spheres. *Nat. Commun.* **2015**, *6*, 8999.

(18) Simmchen, J.; Katuri, J.; Uspal, W. E.; Popescu, M. N.; Tasinkevych, M.; Sánchez, S. Topographical pathways guide chemical microswimmers. *Nat. Commun.* **2016**, *7*, 10598.

(19) Dietrich, K.; Renggli, D.; Zanini, M.; Volpe, G.; Buttinoni, I.; Isa, L. Two-dimensional nature of the active Brownian motion of catalytic microswimmers at solid and liquid interfaces. *New J. Phys.* **2017**, *19*, 065008.

(20) Popescu, M.; Uspal, W.; Dietrich, S. Chemically active colloids near osmotic-responsive walls with surface-chemistry gradients. *J. Phys.: Condens. Matter* **2017**, *29*, 134001.

(21) Singh, D. P.; Choudhury, U.; Fischer, P.; Mark, A. G. Non-equilibrium assembly of light-activated colloidal mixtures. *Adv. Mater.* **2017**, *29*, 1701328.

DOI: 10.1021/acs.jpclett.8b02277
J. Phys. Chem. Lett. 2018, 9, 5023−5028

(22) Dai, B.; Wang, J.; Xiong, Z.; Zhan, X.; Dai, W.; Li, C.-C.; Feng, S.-P.; Tang, J. Programmable artificial phototactic microswimmer. *Nat. Nanotechnol.* **2016**, *11*, 1087.
(23) Nicholls, D.; DeVerse, A.; Esplin, R.; Castañeda, J.; Loyd, Y.; Nair, R.; Voinescu, R.; Zhou, C.; Wang, W.; Gibbs, J. G. Shape-dependent motion of structured photoactive microswimmers. *ACS Appl. Mater. Interfaces* **2018**, *10*, 18050.
(24) Elgeti, J.; Winkler, R. G.; Gompper, G. Physics of microswimmerssingle particle motion and collective behavior: a review. *Rep. Prog. Phys.* **2015**, *78*, 056601.
(25) Palacci, J.; Sacanna, S.; Steinberg, A. P.; Pine, D. J.; Chaikin, P. M. Living crystals of light-activated colloidal surfers. *Science* **2013**, *339*, 936.
(26) Johnson, J. N.; Nourhani, A.; Peralta, R.; McDonald, C.; Thiesing, B.; Mann, C. J.; Lammert, P. E.; Gibbs, J. G. Dynamic stabilization of Janus sphere trans-dimers. *Phys. Rev. E: Stat. Phys., Plasmas, Fluids, Relat. Interdiscip. Top.* **2017**, *95*, 042609.
(27) Wensink, H.; Löwen, H. Aggregation of self-propelled colloidal rods near confining walls. *Phys. Rev. E* **2008**, *78*, 031409.
(28) Takagi, D.; Palacci, J.; Braunschweig, A. B.; Shelley, M. J.; Zhang, J. Hydrodynamic capture of microswimmers into sphere-bound orbits. *Soft Matter* **2014**, *10*, 1784−1789.
(29) Balazs, A. C.; Bhattacharya, A.; Tripathi, A.; Shum, H. Designing bioinspired artificial cilia to regulate particle−surface interactions. *J. Phys. Chem. Lett.* **2014**, *5*, 1691−1700.
(30) Lee, T.-C.; Alarcon-Correa, M.; Miksch, C.; Hahn, K.; Gibbs, J. G.; Fischer, P. Self-propelling nanomotors in the presence of strong Brownian forces. *Nano Lett.* **2014**, *14*, 2407−2412.
(31) Sánchez, S.; Soler, L.; Katuri, J. Chemically powered micro-and nanomotors. *Angew. Chem., Int. Ed.* **2015**, *54*, 1414−1444.
(32) Uspal, W.; Popescu, M.; Tasinkevych, M.; Dietrich, S. Shape-dependent guidance of active Janus particles by chemically patterned surfaces. *New J. Phys.* **2018**, *20*, 015013.
(33) Chiang, T.-Y.; Velegol, D. Localized electroosmosis (LEO) induced by spherical colloidal motors. *Langmuir* **2014**, *30*, 2600−2607.
(34) Wang, W.; Chiang, T.-Y.; Velegol, D.; Mallouk, T. E. Understanding the efficiency of autonomous nano-and microscale motors. *J. Am. Chem. Soc.* **2013**, *135*, 10557−10565.
(35) Walther, A.; Müller, A. H. Janus particles: synthesis, self-assembly, physical properties, and applications. *Chem. Rev.* **2013**, *113*, 5194−5261.
(36) Wittmeier, A.; Leeth Holterhoff, A.; Johnson, J.; Gibbs, J. G. Rotational analysis of spherical, optically anisotropic janus particles by dynamic microscopy. *Langmuir* **2015**, *31*, 10402−10410.
(37) Bharti, B.; Rutkowski, D.; Han, K.; Kumar, A. U.; Hall, C. K.; Velev, O. D. Capillary bridging as a tool for assembling discrete clusters of patchy particles. *J. Am. Chem. Soc.* **2016**, *138*, 14948−14953.
(38) Sullivan, G. M.; Feinn, R. Using effect size−or why the P value is not enough. *J. Grad. Med. Educ.* **2012**, *4*, 279−282.
(39) Axelevitch, A.; Apter, B.; Golan, G. Simulation and experimental investigation of optical transparency in gold island films. *Opt. Express* **2013**, *21*, 4126−4138.
(40) Hong, Y.; Diaz, M.; Córdova-Figueroa, U. M.; Sen, A. Light-driven titanium-dioxide-based reversible microfireworks and micromotor/micropump systems. *Adv. Funct. Mater.* **2010**, *20*, 1568−1576.
(41) Paxton, W. F.; Sundararajan, S.; Mallouk, T. E.; Sen, A. Chemical locomotion. *Angew. Chem., Int. Ed.* **2006**, *45*, 5420−5429.
(42) Brown, A.; Poon, W. Ionic effects in self-propelled Pt-coated Janus swimmers. *Soft Matter* **2014**, *10*, 4016−4027.
(43) Ebbens, S.; Gregory, D.; Dunderdale, G.; Howse, J.; Ibrahim, Y.; Liverpool, T.; Golestanian, R. Electrokinetic effects in catalytic platinum-insulator Janus swimmers. *Europhys. Lett.* **2014**, *106*, 58003.
(44) Paxton, W. F.; Baker, P. T.; Kline, T. R.; Wang, Y.; Mallouk, T. E.; Sen, A. Catalytically induced electrokinetics for motors and micropumps. *J. Am. Chem. Soc.* **2006**, *128*, 14881−14888.
(45) Giesbers, M.; Kleijn, J. M.; Cohen Stuart, M. A. The electrical double layer on gold probed by electrokinetic and surface force measurements. *J. Colloid Interface Sci.* **2002**, *248*, 88−95.
(46) Gu, Y.; Li, D. The ζ-potential of glass surface in contact with aqueous solutions. *J. Colloid Interface Sci.* **2000**, *226*, 328−339.
(47) Wilhelm, P.; Stephan, D. Photodegradation of rhodamine B in aqueous solution via SiO_2@TiO_2 nano-spheres. *J. Photochem. Photobiol., A* **2007**, *185*, 19−25.
(48) Mann, C. J.; Yu, L.; Lo, C.-M.; Kim, M. K. High-resolution quantitative phase-contrast microscopy by digital holography. *Opt. Express* **2005**, *13*, 8693−8698.
(49) Kim, D.; Darve, E. Molecular dynamics simulation of electro-osmotic flows in rough wall nanochannels. *Phys. Rev. E* **2006**, *73*, 051203.
(50) Messinger, R.; Squires, T. Suppression of electro-osmotic flow by surface roughness. *Phys. Rev. Lett.* **2010**, *105*, 144503.
(51) Robbie, K.; Brett, M. Sculptured thin films and glancing angle deposition: Growth mechanics and applications. *J. Vac. Sci. Technol., A* **1997**, *15*, 1460−1465.
(52) Mark, A. G.; Gibbs, J. G.; Lee, T.-C.; Fischer, P. Hybrid nanocolloids with programmed three-dimensional shape and material composition. *Nat. Mater.* **2013**, *12*, 802.
(53) Jeong, H.-H.; Mark, A. G.; Gibbs, J. G.; Reindl, T.; Waizmann, U.; Weis, J.; Fischer, P. Shape control in wafer-based aperiodic 3D nanostructures. *Nanotechnology* **2014**, *25*, 235302.
(54) Choudhury, U.; Soler, L.; Gibbs, J. G.; Sanchez, S.; Fischer, P. Surface roughness-induced speed increase for active Janus micromotors. *Chem. Commun.* **2015**, *51*, 8660−8663.
(55) Dolatshahi-Pirouz, A.; Hovgaard, M. B.; Rechendorff, K.; Chevallier, J.; Foss, M.; Besenbacher, F. Scaling behavior of the surface roughness of platinum films grown by oblique angle deposition. *Phys. Rev. B: Condens. Matter Mater. Phys.* **2008**, *77*, 115427.
(56) O'Neel-Judy, E.; Nicholls, D.; Castañeda, J.; Gibbs, J. G. Light-activated, multi-semiconductor hybrid microswimmers. *Small* **2018**, *14*, 1801860.
(57) Dunderdale, G.; Ebbens, S.; Fairclough, P.; Howse, J. Importance of particle tracking and calculating the mean-squared displacement in distinguishing nanopropulsion from other processes. *Langmuir* **2012**, *28*, 10997−11006.

DOI: 10.1021/acs.jpclett.8b02277
J. Phys. Chem. Lett. 2018, 9, 5023−5028